Ann. Geophys. Discuss., https://doi.org/10.5194/angeo-2019-23
Manuscript under review for journal Ann. Geophys.
Discussion started: 14 March 2019

Annales Geophysicae Discussions Open Access EGU

Variation in altitude of high-frequency enhanced plasma line by the pump near the 5th electron gyro-harmonic

Jun Wu[a*], Jian Wu[a], Michael. T. Rietveld[b] , Ingemar. Haggstrom[c] , Haisheng Zhao[a], Tong Xu[a], Zhengwen Xu[a]

[a]*National Key laboratory of electromagnetic environment, China research institute of radio wave propagation, Beijing, 102206, China*

[b]*EISCAT Scientific Association, 9027 Ramfjordbotn, Norway*

[c]*EISCAT Scientific Association, SE-981 92 Kiruna, Sweden*

Abstract

During an ionospheric heating campaign carried out at the European Incoherent Scatter Scientific Association (EISCAT), the ultra high frequency incoherent scatter (IS) radar observed a systematic variation in the altitude of the high-frequency enhanced plasma line (HFPL), which behaves depending on the pump frequency. Specifically, the HFPL altitude becomes lower when the pump lies above the 5th gyro-harmonic. The analysis shows that the enhanced electron temperature plays a decisive role in the descent in the HFPL altitude. That is, on the traveling path of the enhanced Langmuir wave, the enhanced electron temperature can only be matched by the low electron density at a lower altitude so that the Bragg condition can be satisfied, as expected from the dispersion relation of Langmuir wave.

Keywords: ionospheric heating, incoherent scatter radar, enhanced plasma line, altitude, Bragg condition.

Ann. Geophys. Discuss., https://doi.org/10.5194/angeo-2019-23
Manuscript under review for journal Ann. Geophys.
Discussion started: 14 March 2019

1. Introduction

The oscillation two stream instability (OTSI) and the parametric decay instability (PDI) have been extensively investigated [Silin 1965; DuBois and Goldman 1965, 1967; Perkins and Flick 1971; Rosenbluth 1972; Drake et al.,, 1974; Perkins, et al.,, 1974; Kuo and Cheo 1978; Wu et al.,, 2006; Wu et al.,, 2007). As the signatures of the PDI and OTSI, the high-frequency enhanced plasma line (HFPL) and the high-frequency enhanced ion line (HFIL) are observed by the incoherent scattering (IS) radar during the ionospheric heating campaign. Using those observations of IS radar, the IS spectrum (Kuo and Fejer, 1972; Stubbe et al., 1992; Kohl et al., 1993; Carlson et al., 1972; Gordon and Carlson,1974; Kantor, 1974; Hagfors et al., 1983; Dubois et al., 1988; Nordling et al., 1988 ; Stubbe et al., 1985), the pump threshold for the PDI and OTSI (Fejer, 1979; Bezzerides and Weinstock, 1972; Weinstock and Bezzerides, 1972), the temporal properties of the PDI and OTSI (Kohl et al., 1993; Gordon and Carlson, 1974; Kantor, 1974; Stubbe et al., 1985; Carlson et al., 1972; Jones et al., 1986) and the altitude properties of the HFPL and HFIL (Stubbe et al., 1992 ; Kohl et al., 1987, 1993; Djuth et al., 1994; Ashrafi et al., 2006; Wu et al., 2017a, 2018b) were examined.

The enhanced Langmuir wave and ion acoustic wave are usually excited in the altitude range from the reflection altitude of the pump to the altitude where the heavy Landau effect on Langmuir wave may take place (Stubbe et al., 1992). However, the enhanced Langmuir wave and ion acoustic wave can't be observed by IS radar in the exciting altitude range, but at an altitude where the Bragg condition is satisfied

Ann. Geophys. Discuss., https://doi.org/10.5194/angeo-2019-23
Manuscript under review for journal Ann. Geophys.
Discussion started: 14 March 2019

(Stubbe et al., 1992; Kohl et al., 1987, 1993). Some usual observations of the ultra high frequency (UHF) radar at European Incoherent Scatter Scientific Association (EISCAT) show that the HFIL altitude is about ~ 3 km – ~ 5 km higher than the HFPL altitude (Stubbe et al., 1992; Kohl et al., 1993). Additionally, the altitude extending of ~ 3 km – ~ 5 km frequently appears in the power profile of the HPIL, but does not in the power profile of the HFPL (Stubbe et al., 1992; Kohl et al., 1993). Moreover, some observations at EISCAT illustrated that a descent in the altitude of the plasma turbulence took place over tens of seconds after the pump on, which was most likely attributed to the modification in electron density by the ionospheric heating (Djuth et al., 1994). UHF radar at EISCAT observed the descent in the HFIL altitude from ~ 230 km to ~ 220 km within ~ 60 s, which was also attributed to the modification in electron density (Ashrafi et al., 2006).

Although those variations in the HFPL and HFIL altitudes were attributed to the enhanced electron temperature and the modified electron density, the dominant one of which was not clearly identified (Wu et al., 2017a). Furthermore, it was identified that the enhanced electron temperature dominated over the modified electron density in the variation in the HFIL altitude (Wu et al., 2018b). As a further work, this paper examines the variation in the HFPL altitude in more detail. Indeed, the dispersion behavior of Langmuir wave is very different from that of ion acoustic wave.

2. Experiment and data

An ionospheric heating campaign was performed at EISCAT at 12:32:30 UT – 14:30 UT (universal time) on Mar. 11, 2014. The experiment arrangement has been

Ann. Geophys. Discuss., https://doi.org/10.5194/angeo-2019-23
Manuscript under review for journal Ann. Geophys.
Discussion started: 14 March 2019

described in more detail by Wu et al., (2016, 2017b). Briefly, the EISCAT heater (Rietveld et al., 1993, 2016) radiated the O mode pump in the frequency band of 6.7 MHz – 7 MHz, and the UHF IS radar was operated as the leading diagnostic means. The pump frequency f_{HF} was stepped down and up in a step of 2.804 kHz with a period of 10 s as shown in those bottom panels in **Figure 1, Figure 2** and **Figure 3**. During the experiment, the local geomagnetic was relatively quiet. At an altitude of 200 km, the total geomagnetic varied in the range of 49202 nT – 49233 nT.

Considering the variation in the intensity of ion line, we adopt a convention for the following discussion: the f_{HF} band of 6.7 MHz – 7 MHz can be divided into three daughter bands, that is, the higher band (HB, above $5f_{ce}$), the gyro-harmonic band (GB, very close to $5f_{ce}$) and lower band (LB, below $5f_{ce}$), where f_{ce} represents the electron gyro-frequency (Wu et al., 2016, 2017a, 2017b, 2018a, 2018b, 2019). For instance, in the 1st heating cycle, the HB is set as 7 MHz – ~ 6.871028 MHz, the GB as ~ 6.868224 MHz – ~ 6.837383 MHz and the LB as ~ 6.834579 MHz – 6.7 MHz, which temporally correspond to the time intervals of 12:30:00 UT – 12:37:40 UT, 12:37:50 UT – 12:39:40 UT and 12:39:50 UT – 12:48:00 UT, respectively. Actually, the frequency division in each heating cycle should be somewhat different from each other due to the slight disturbance of the geomagnetic.

From the 1st panel to the 6th panel in **Figure 1**, the normalized plasma lines at those altitudes of 210.25 km, 207.32 km, 204.39 km, 201.45 km, 198.52 km and 195.58 km are successively given, which lie in the frequency range of -6.7 MHz – –7.25 MHz. One can find that those HFPLs in the GB and HB lie at frequency

Ann. Geophys. Discuss., https://doi.org/10.5194/angeo-2019-23
Manuscript under review for journal Ann. Geophys.
Discussion started: 14 March 2019

$f_{\mathrm{HF}} - 9.45\mathrm{kHz}$ as the expected decay line from the PDI. In the GB, those strong HFPLs of up to ~ 1 occur at an altitude of 201.45 km in the 1st heating cycle, at an altitude of 210.25 km in the 2nd heating cycle and at an altitude of 207.32 km in the 3rd and 4th heating cycles respectively. In the HB, however, those strong HFPLs of up to ~ 1 descend in altitude, that is, they are located at an altitude of 198.52 km in the 1st heating cycle, at altitudes of 207.32 km and 204.39 km in the 2nd heating cycle, at an altitude of 204.39 km in the 3rd and 4th heating cycles. On the other hand, in the LB, the HFPL has not appeared at any of those altitudes due to the absence of the PDI and OTSI (Wu et al., 2019).

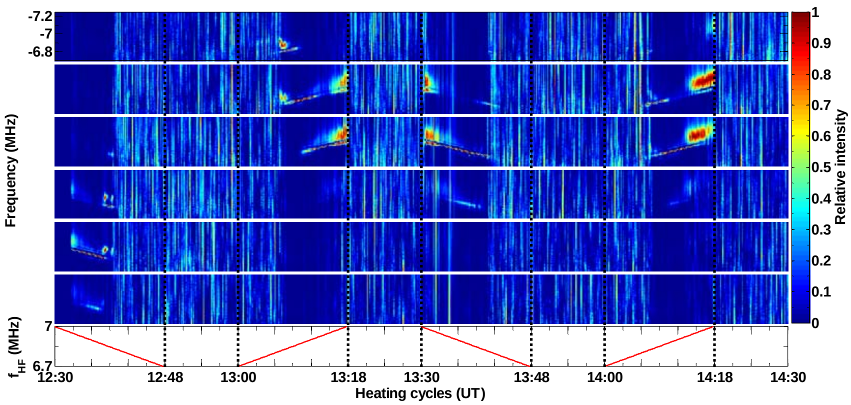

Figure 1. The plasma lines versus f_{HF} (the heating cycles), where the 1st panel is for an altitude of 210.25 km, the 2nd panel for 207.32 km , the 3rd panel for 204.39 km, the 4th panel for 201.45 km, the 5th panel for 198.52 km, the 6th panel for 195.58 km and the 7th panel for f_{HF} (the heating cycles), successively from top to bottom.

Figure 2 gives the altitude profile of $T_{\mathrm{e}}/T_{\mathrm{e0}}$ as a function of f_{HF}, where T_{e} is the electron temperature and T_{e0} the undisturbed electron temperature. At an altitude of ~ 200 km, $T_{\mathrm{e}}/T_{\mathrm{e0}}$ immediately enhances when heating on, and obviously varies with f_{HF}. $T_{\mathrm{e}}/T_{\mathrm{e0}}$ strongly enhances up to ~ 1.5 in the LB, whereas it slightly enhances up to ~ 1.25 in the HB. In the GB, T_e/T_{e0} approximately reach ~ 1.2. Evidently, $(T_e/T_{e0})_{LB} > (T_e/T_{e0})_{HB} > (T_e/T_{e0})_{GB}$, where $(T_e/T_{e0})_{LB}$, $(T_e/T_{e0})_{HB}$ and $(T_e/T_{e0})_{GB}$ represent T_e/T_{e0} in the LB, HB and GB respectively. This variation in T_e/T_{e0} depends on the dispersion behavior of the excited upper hybrid waves at the upper hybrid altitude (Wu et al., 2017b), where is ~ 2 km – ~ 10 km below the reflection altitude of the pump (Gurevich, 2007).

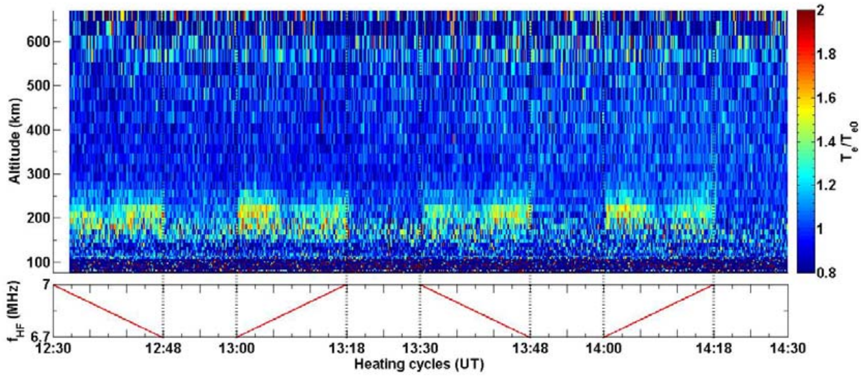

Figure 2. T_e/T_{e0} versus f_{HF} (the heating cycles), where T_{e0} is obtained by averaging the electron temperature over the final 5 minutes of the UHF radar observations at 14:25 UT – 14:30 UT.

Figure 3 is the altitude profile of N_e/N_{e0} as a function of f_{HF}, where N_e is the electron density and N_{e0} the undisturbed electron density. In the 3rd and 4th heating cycles, the enhanced N_e/N_{e0} of up to ~ 1.4 take place in the GB and HB and can be seen in a narrow region around an altitude of ~ 200 km. In accordance with the standard IS analysis, the enhanced N_e/N_{e0} should not correspond to the real enhancement in the electron density, but to the HFIL excited by the PDI and OTSI (Wu et al., 2017b). On the other hand, no apparent enhancement in N_e/N_{e0} takes place around an altitude of ~ 200 km in the 1st and 2nd heating cycles. This may be due to

Ann. Geophys. Discuss., https://doi.org/10.5194/angeo-2019-23
Manuscript under review for journal Ann. Geophys.
Discussion started: 14 March 2019

the high background electron density and the ambiguity of radar measurement (Wu et al., 2017b). Additionally, the enhanced N_e/N_{e0} appears over a wide altitude range of ~ 250 km – ~ 670 km, which is hardly explained by the standard IS analysis and is open (Wu et al., 2017b).

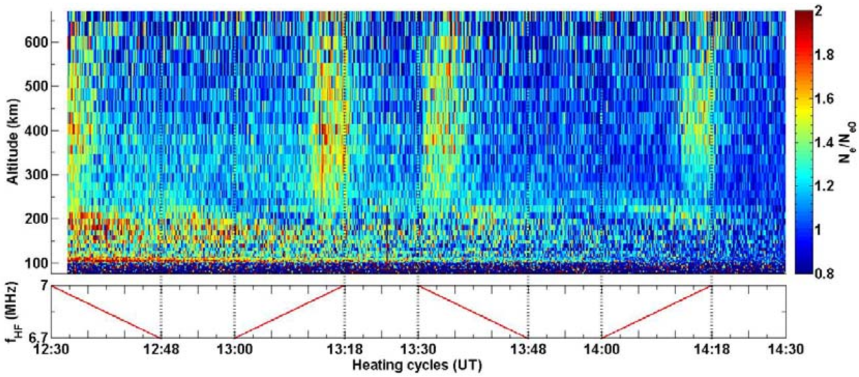

Figure 3. N_e/N_{e0} versus f_{HF} (the heating cycles), where N_{e0} is obtained by averaging the electron density over the final 5 minutes of the UHF radar observations at 14:25 UT – 14:30 UT.

In summary, **Figure 1** shows that (1) the HFPL altitude in the 1st heating cycle is far lower than that in the 2nd, 3rd and 4th heating cycles; (2) interestingly enough, those HFPL altitudes in the GB and HB systematically vary with f_{HF}, that is, the HFPL altitude in the HB is slightly lower than that in the GB. Additionally, **Figure 2** implies that T_e also systematically varies with f_{HF}, whereas N_e does not as illustrated in **Figure 3**.

3. Discussion

OTSI and PDI can be excited in the altitude range of (Stubbe et al., 1992)

$$h_0 - 0.1H \le h_{ex} < h_0 \quad (1)$$

where h_0 is the reflection altitude of the pump, H is the scale altitude and h_{ex} is

Ann. Geophys. Discuss., https://doi.org/10.5194/angeo-2019-23
Manuscript under review for journal Ann. Geophys.
Discussion started: 14 March 2019

the exciting altitude of the PDI and OTSI. For a typical ionosphere, due to the monotonous change in the profile of N_e below the ionospheric peak, h_{ex} in the HB should be higher than that in the GB. In **Figure 3**, it is evident that N_e/N_{e0} in the 1st heating cycle reaches ~ 1.7 near an altitude of 200 km and is far larger than that in the 2nd, 3rd and 4th heating cycles. This implies that h_0 in the 1st heating cycle should be far lower than that in the 2nd, 3rd and 4th heating cycles. Correspondingly, h_{ex} and the HFPL altitude in the 1st heating cycle should be far lower than that in the 2nd, 3rd and 4th heating cycles.

However, function (1) fails to explain that the HFPL altitude in the HB is slightly lower than that in the GB. Considering an field-aligned and monostatic operating observation, the enhanced Langmuir wave traveling in a non-uniform and stationary ionosphere should satisfy the dispersion relation (Kohl et al., 1993)

$$\omega_L^2 = \omega_{pe}^2 + \gamma \frac{K_B T_e}{m_e} k_L^2 \quad (2)$$

where ω_L is the angular frequency of Langmuir wave, ω_{pe} is the Langmuir angular frequency of ionospheric plasma, γ is the adiabatic index, K_B is the Boltzmann constant, k_L is the wave number of Langmuir wave, and m_e is the electron mass.

When the enhanced Langmuir wave travels in a non-uniform and stationary ionosphere, k_L may change, whereas ω_L will not change. That is, k_L should depend on ω_{pe} and T_e on the traveling path of the enhanced Langmuir wave, as expected from function (2). This implies that at a particular altitude, k_L will satisfies the Bragg condition, namely, $k_L = 2k_r$, and the enhanced Langmuir wave should be observed by radar, where k_r is the wave number of radar. Then, considering $T_e = T_e'$,

Ann. Geophys. Discuss., https://doi.org/10.5194/angeo-2019-23
Manuscript under review for journal Ann. Geophys.
Discussion started: 14 March 2019

Annales Geophysicae Discussions
Open Access
EGU

the enhanced Langmuir wave should be observed at an altitude of h' where $2k_{\mathrm{r}} = k_{\mathrm{L}} = \sqrt{\dfrac{\left(\omega_{\mathrm{L}}^2 - \omega_{\mathrm{pe}}'^2\right) m_{\mathrm{e}}}{\gamma \mathrm{K_B} T_{\mathrm{e}}'}}$, which is a derivation of function (2). On the other hand, $T_{\mathrm{e}} = T_{\mathrm{e}}''$ is considered, then the enhanced Langmuir wave should be observed at other altitude of h'', where $2k_{\mathrm{r}} = k_{\mathrm{L}} = \sqrt{\dfrac{\left(\omega_{\mathrm{L}}^2 - \omega_{\mathrm{pe}}''^2\right) m_{\mathrm{e}}}{\gamma \mathrm{K_B} T_{\mathrm{e}}''}}$. Obviously, $\dfrac{\omega_{\mathrm{L}}^2 - \omega_{\mathrm{pe}}''^2}{T_{\mathrm{e}}''} = \dfrac{\omega_{\mathrm{L}}^2 - \omega_{\mathrm{pe}}'^2}{T_{\mathrm{e}}'}$ can be obtained. Furthermore, if $T_{\mathrm{e}}'' > T_{\mathrm{e}}'$, then $\omega_{\mathrm{pe}}'' < \omega_{\mathrm{pe}}'$. Due to the monotonous profile of ω_{pe} below the ionospheric peak, $h'' < h'$ will be obtained. In other word, on the traveling path of the enhanced Langmuir wave, the higher T_{e} is, the lower the observing altitude of the enhanced Langmuir wave is. The fact is $\left(T_{\mathrm{e}}/T_{\mathrm{e0}}\right)_{\mathrm{HB}} > \left(T_{\mathrm{e}}/T_{\mathrm{e0}}\right)_{\mathrm{GB}}$ as shown in Figure 2. As a result, the HFPL altitude in the HB should be lower than that in the GB as shown in Figure 1.

As an example, the HFPL in the 4th heating cycle is examined. The left panel of **Figure 4** respectively gives the profiles of $\omega_{\mathrm{L}}^2 - \omega_{\mathrm{pe}}^2$, T_{eGB} and T_{eHB} in the altitude range of 190 km – 230 km in the 4th heating cycle. Here, the profile of $\omega_{\mathrm{L}}^2 - \omega_{\mathrm{pe}}^2$ is not distinguished in the GB and HB, implying an assumption that the profiles of N_{e} was not modified by the ionospheric heating. Indeed, it is difficult to measure the slight modification in electron density due to (1) N_{e} is much variable in space and time, and (2) the artificial modification in N_{e} is relatively small (Rietveld et al., 2003). Also, **Figure 3** really exhibits that no real modification in $N_{\mathrm{e}}/N_{\mathrm{e0}}$ is induced by the ionospheric heating in the altitude range examined (Wu et al., 2017b). Obviously, $\omega_{\mathrm{L}}^2 - \omega_{\mathrm{pe}}^2$ monotonically decreases with the ascent in altitude and has a vertical gradient of $\sim -3.1\times10^{15}\ \mathrm{rad^2 s^2 km^{-1}}$ in the altitude range of 200 km – 230

Ann. Geophys. Discuss., https://doi.org/10.5194/angeo-2019-23
Manuscript under review for journal Ann. Geophys.
Discussion started: 14 March 2019

km. Moreover, $\omega_{\mathrm{L}}^2-\omega_{\mathrm{pe}}^2$ becomes negative above an altitude of ~ 208.5 km due to the increasing N_{e} with the ascent in altitude. In addition, the profile of T_{eGB} demonstrates the gradient of ~ 6.09 Kkm^{-1} within the altitude range of 190 km – 200 km and ~ – 8.85 Kkm^{-1} within the altitude range of 200 km – 230 km, whereas T_{eHB} demonstrates the gradient of ~ 40.82 Kkm^{-1} within the altitude range of 190 km – 200 km and ~ – 17.77 Kkm^{-1} within the altitude range of 200 km – 230 km. This implies that the strongest enhancement in T_{e} takes place an altitude of ~ 200 km and the thermal energy should be conducted along the magnetic field within an extending altitude range.

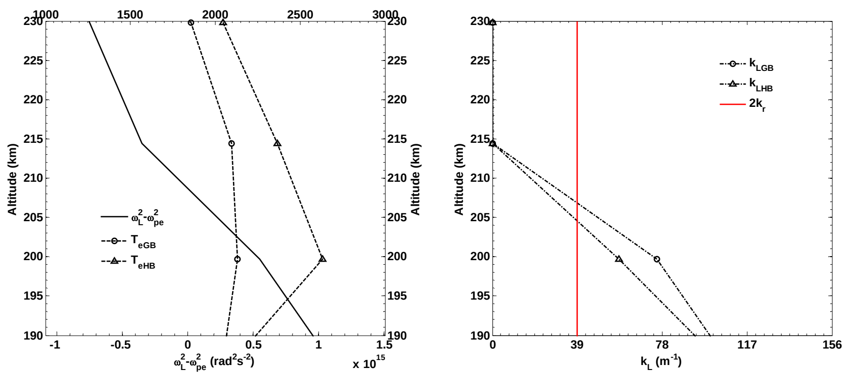

Figure 4. The altitude profiles of $\omega_{\mathrm{L}}^2-\omega_{\mathrm{pe}}^2$, T_{eGB}, T_{eHB} (the left panel), k_{LGB}, k_{LHB} and k_{r} (the right panel), where $\omega_{\mathrm{L}}=2\pi\times6.8$ MHz, $\omega_{\mathrm{pe}}=2\pi\times8.9\sqrt{N_e}$, N_{e} is obtained by averaging over the time interval of [14:07:20 UT, 14:09:10 UT], T_{eGB} and T_{eHB} are obtained by averaging over the time intervals of [14:07:20 UT, 14:09:10 UT] and [14:11:20 UT, 14:18:00 UT], respectively, and $k_{\mathrm{r}}=19.5\ \mathrm{m}^{-1}$ is the wave number of EISCAT UHF radar.

In the right panel of **Figure 4**, the profiles of k_{LGB} and k_{LHB} in the altitude range of 190 km – 230 km in the 4th heating cycle are demonstrated, where k_{LGB} and k_{LHB} represent the wave numbers of the enhanced Langmuir wave in the GB and HB. The profile of k_{LGB} has a gradient of $\sim -2.78\ \mathrm{m^{-1}km^{-1}}$ within the altitude range of 190 km – 200 km and $\sim -5.1\mathrm{m^{-1}km^{-1}}$ within the altitude range of 200 km – 214.4 km, and $k_{\mathrm{LGB}} = 2k_{\mathrm{r}}$ takes place at an altitude of ~ 206.8 km. Moreover, the profile of k_{LHB} demonstrates a gradient of $\sim -3.15\ \mathrm{m^{-1}km^{-1}}$ within an altitude range examined, and $k_{\mathrm{LHB}} = 2k_{\mathrm{r}}$ at an altitude of ~ 204.5 km. This indicates that the enhanced T_{e} on the traveling path can remarkably impact on k_{L}, and the enhanced Langmuir waves in the GB and HB should be observed at different altitude, namely, ~ 206.8 km in the GB and ~ 204.5 km in the HB respectively. Thus, the altitude difference between the HFPL altitudes in the GB and HB is 2.3 km as illustrated in the right panel of **Figure 4**. Taking the height resolution of ~ 3 km of EISCAT UHF radar into account, the HFPL altitudes in the GB and HB in the 4th heating cycle shown in **Figure 1** are in perfect agreement with the altitudes of $k_{\mathrm{LGB}} = 2k_{\mathrm{r}}$ and $k_{\mathrm{LHB}} = 2k_{\mathrm{r}}$ illustrated in the right panel of **Figure 4**. In addition, k_{LGB} and k_{LHB} become zero above an altitude of ~ 208.5, implying the enhanced Langmuir wave will be reflected at an altitude of ~ 208.5 km.

Usually, ω_{pe} is on the order of 10^6 and $\sqrt{\gamma \frac{K_{\mathrm{B}} T_{\mathrm{e}}}{m_{\mathrm{e}}}} k_{\mathrm{L}}$ is on the order of 10^3 for a typical ionosphere, implying that N_{e} dominates over T_{e} in k_{L}. However, this does not imply that the enhanced T_{e} is independent of the HFPL altitude. Indeed, on the traveling path of Langmuir wave, an remarkable enhancement in electron temperature owing to an ionospheric heating will take significant impact on k_{L}. For a

Ann. Geophys. Discuss., https://doi.org/10.5194/angeo-2019-23
Manuscript under review for journal Ann. Geophys.
Discussion started: 14 March 2019

large gradient profile of N_e, an somewhat enhancement in T_e may lead to an remarkable descent in the HFPL altitude. Moreover, if a small gradient profile of N_e is considered, that is, N_e can be approximately considered as a constant, then k_L will be mainly determined by the profile of T_e.

4. Conclusions

A systematic variation in the HFPL altitude induced by the pump near the 5th gyro-harmonic at EISCAT, is paid attention. The IS radar observation demonstrates that the HFPL altitude and the electron temperature behave as a function of the pump frequency. More specifically, when the pump frequency approaches the 5th gyro-harmonic from below, the electron temperature is somewhat enhanced, and the HFPL is observed at an altitude as expected. When the pump frequency sweeps above the 5th gyro-harmonic, however, the electron temperature is prominently enhanced, and the HFPL altitude slightly plunge downward.

In conclusion, the HFPL altitude is dependent on the dispersion behavior of the enhanced Langmuir wave and the Bragg condition, and is determined by the profiles of the electron density and the enhanced electron temperature. When heating above the 5th gyro-harmonic, the HFPL altitude plunge downward owing to the thermal effect of ionospheric heating on the traveling path of the enhanced Langmuir wave. In other word, when the pump sweeps above the 5th gyro-harmonic, the IS radar should observe the enhanced Langmuir wave at an lower altitude, where the low electron density can compensate the remarkably enhanced electron temperature so that the Bragg condition can be satisfied, as expected by the dispersion relation of Langmuir

Ann. Geophys. Discuss., https://doi.org/10.5194/angeo-2019-23
Manuscript under review for journal Ann. Geophys.
Discussion started: 14 March 2019

wave.

Acknowledgments

We would like to thank the engineers of EISCAT in Tromsø for keeping the facility in excellent working condition and Tromsø Geophysical Observatory, UiT The Arctic University of Norway, for providing the magnetic data of Tromsø recorded on 11 Mar. 2014. The data of UHF radar can be obtained freely from EISCAT (http://www.eiscat.se/schedule/schedule.cgi). The EISCAT Scientific Association is supported by China (China Research Institute of Radiowave Propagation), Finland (Suomen Akatemia of Finland), Japan (the National Institute of Polar Research of Japan and Institute for Space-Earth Environmental Research at Nagoya University), Norway (Norges Forkningsrad of Norway), Sweden (the Swedish Research Council) and the UK (the Natural Environment Research Council).

References

Ashrafi M., Kosch, M. J., and Honary, F.: Heater-induced altitude descent of the EISCAT UHF ion line enhancements: Observations and modeling, Advances in Space Research, 38, 2645-2652, https://doi.org/10.1016/j.asr.2005.06.079 , 2006.

Bezzerides, B. and Weinstock, J.: Nonlinear saturation of parametric instabilities, Phys. Rev. Lett., 28, 481- 484, https://doi.org/10.1103/PhysRevLett.28.481, 1972.

Carlson, H. C., Gordon, W. E., and Showen, R. L.: High frequency induced enhancements of the incoherent scatter spectrum at Arecibo, J. Geophys. Res., 77, 7, 1242-1250, https://doi.org/10.1029/JA077i007p01242,1972.

Djuth, F. T., Stubbe, P., Kohl, H. W., Rietveld, M. T., and Elder, J. H.: Altitude characteristics of plasma turbulence excited with the Tromsø Superheater, J. Geophys. Res., 99, 333-339, https://doi.org/10.1029/93JA02289, 1994.

Drake, J. F., Lee, Y. C., Schmid, G., Liu, C. S., and Rosenbluth, M. N.: Parametric instabilities of electromagnetic waves in plasmas, Phys. Fluids, 17, 778-785, https://doi.org/10.1063/1.1694789, 1974.

Dubois D. F., Rose, H., and Russell, D.: Power spectra of fluctuations in strong Langmuir turbulence, Phys. Rev. Lett., 61, 2209-2212, https://doi.org/10.1103/PhysRevLett.61.2209, 1988.

DuBois, D. F. and Goldman M. V.: Parametrically excited plasma fluctuations, Phys. Rev., 164, 207-222, https://doi.org/10.1103/PhysRev.164.207, 1967.

DuBois, D. F. and Goldman, M. V.: Radiation induced in stability of electron plasma oscillations, Phys. Rev. Lett., 14, 544-546, https://doi.org/10.1103/PhysRevLett.14.544 , 1965.

Fejer, J. A.: Ionospheric modification and parametric instabilities, Reviews of Geophysics and space physics, 17, 135-153, https://doi.org/10.1029/RG017i001p00135, 1979.

Gordon, W. E. and Carlson, H. C.: Arecibo heating experiments, Radio Sci., 9, 1041-1047, https://doi.org/10.1029/RS009i011p01041, 1974.

Gurevich, A. V.: Nonlinear effects in the ionosphere, Physics Uspekhi, 50, 1091-1121, https://doi.org/10.1070/PU2007v050n11ABEH006212, 2007.

Hagfors, T., Kofman, W., Kopka, H., and Stubbe, P.: Observations of enhanced plasma lines by EISCAT during heating experiments, Radio Sci., 18, 861-866, https://doi.org/10.1029/RS018i006p00861, 1983.

Jones, T. B., Robinson, T. R., Stubbe, P., and Kopka, H.: EISCAT observations of the heated ionosphere, J. Atmosph. Terr. Phys., 48, 1027-1035, https://doi.org/10.1016/0021-9169(86)90074-7, 1986.

Kantor, I. J.: High frequency induced enhancements of the incoherent scatter spectrum at Arecibo. II, J. Geophys. Res., 79, 199-208, https://doi.org/10.1029/JA079i001p00199,1974.

Kohl, H. W., Kopka, H., Lahoz, C., and Stubbe, P.: Propagation of artificially excited Langmuir waves in the ionosphere, Radio Sci., 22, 655-661, https://doi.org/10.1029/RS022i004p00655, 1987.

Kohl, H., Kopka, H., Stubbe, P., and Rietveld, M. T.: Introduction to ionospheric

Ann. Geophys. Discuss., https://doi.org/10.5194/angeo-2019-23
Manuscript under review for journal Ann. Geophys.
Discussion started: 14 March 2019

heating experiments at Tromsø-II. Scientific problems, J. Atmos. Terr. Phys., 55, 601-603, https://doi.org/10.1016/0021-9169(93)90008-M, 1993.

Kuo, S. P. and Chen, B. R.: Parametric excitation of coupled plasma waves, Phys. Fluids, 21, 1753-1757, https://doi.org/10.1063/1.862091, 1978.

Kuo, Y. Y. and Fejer, J. A.: Spectral-line structures of saturated parametric instabilities, Phys. Rev. Lett., 29, 1667-1670, https://doi.org/10.1103/PhysRevLett.29.1667, 1972.

Nordling, J., Hedberg, A., Wannberg, G., Leyser, T. B., Derblom, H., Opgenoorth, H. J., and Lahoz, C.: Simultaneous bistatic European Incoherent Scatter UHF, 145 - MHz radar and stimulated electromagnetic emission observations during HF ionospheric modification, Radio Sci., 23, 809-819, https://doi.org/10.1029/RS023i005p00809, 1988.

Perkins F. W. and Flick J.: Parametric Instabilities in Inhomogeneous Plasmas, Phys. Fluids, 14, 2012-2018, https://doi.org/10.1063/1.1693711, 1971.

Perkins, F. W., Oberman, C., and Valeo, E. J.: Parametric instabilities and ionospheric modification, J. Geophys. Res., 79, 1478-1496, https://doi.org/10.1029/JA079i010p01478, 1974.

Rietveld, M. T. , Kosch, M. J., Blagoveshchenskaya, N. F., Kornienko, V. A., and Yeoman, T. K.: Ionospheric electron heating, optical emissions, and striations induced by powerful hf radio waves at high latitudes: aspect angle dependence, J. Geophys. Res., 108, 1141-1156, https://doi.org/10.1029/2002JA009543, 2003.

Rietveld, M. T., Kohl, H., Kopka, H., and Stubbe, P.: Introduction to ionospheric heating at Tromsø-I. Experimental overview, J. Atmos. Terr. Phys., 55, 577-599, https://doi.org/10.1016/0021-9169(93)90007-L, 1993.

Rietveld, M. T., Senior, A., Markkanen, J., and Westman, A.: New capabilities of the upgraded EISCAT high-power HF facility, Radio Sci., 51, 1533-1546, https://doi.org/10.1002/2016RS006093, 2016.

Rosenbluth, M. N.: Parametric instabilities in inhomogeneous media, Phys. Rev. Lett., 29, 565-567, https://doi.org/10.1103/PhysRevLett.29.565, 1972.

Silin, V. P.: Parametric resonance in a plasma, Sov. Phys. JETP, Engl. Transl., 21, 1127-1134, 1965.

Ann. Geophys. Discuss., https://doi.org/10.5194/angeo-2019-23
Manuscript under review for journal Ann. Geophys.
Discussion started: 14 March 2019

Stubbe P., Kohl, H., and Rietveld, M. T.: Langmuir turbulence and ionospheric modification, J. Geophys. Res., 97, 6285-6297, https://doi.org/10.1029/91JA03047, 1992.

Stubbe P., Kopka, H., Rietveld, M. T., Frey, A., Høeg, P., Kohl, H., Nielsen, E., and Rose, G.: Ionospheric modification experiments with the Tromsø heating facility, J. Atmos. Terr. Phys., 47, 1151-1163, https://doi.org/10.1016/0021-9169(85)90085-6, 1985.

Weinstock, J. and Bezzerides, B.: Threshold of ionospheric modifications by radio waves, J. Geophys. Res., 77, 761-764, https://doi.org/10.1029/JA077i004p00761, 1972.

Wu J., Wu, J., and LaHoz, C.: On the ponderomotive force and the effect of loss reaction on parametric instability, Chinese Physics, 16, 558-563, https://doi.org/10.1088/1009-1963/16/2/046, 2007.

Wu J., Wu, J., Rietveld, M. T., Haggstrom, I., Zhao, H., and Xu, Z.: Altitude and intensity characteristics of parametric instability excited by an HF pump wave near the fifth electron harmonic, Plasma Sci. Technol., 19, 125303(7pp), https://doi.org/10.1088/2058-6272/aa9027, 2017a

Wu, J., Wu, J., Rietveld, M. T., Haggstrom, I., Xu, Z., zhang, Y., Xu, T., and Zhao, H.: The intensities of high frequency - enhanced plasma and ion lines during ionospheric heating, J. Geophys. Res., 124, 603-615, https://doi.org/10.1029/2018JA025918, 2019.

Wu, J., Wu, J., Rietveld, M. T., Haggstrom, I., Xu, Z., and Zhao, H.: The extending of observing altitudes of plasma and ion lines during ionospheric heating, J. Geophys. Res., 123, 918-930, https://doi.org/10.1002/2017JA024809, 2018a.

Wu, J., Wu, J., Rietveld, M. T., Haggstrom, I., Zhao, H., Xu, T., and Xu, Z.: Systematic variation in observing altitude of enhanced ion line by the pump near fifth gyroharmonic, Plasma Sci. Technol., 20, 125301(8pp), https://doi.org/10.1088/2058-6272/aadd44, 2018b.

Wu, J., Wu, J., Rietveld, M. T., Haggstrom, I., Zhao, H., and Xu, Z.: The behavior of electron density and temperature during ionospheric heating near the fifth electron gyrofrequency, J. Geophys. Res., 122, 1277-1295, https://doi.org/10.1002/2016JA023121, 2017b.

Wu, J., Wu, J., and Xu, Z.: Results of ionospheric heating experiments involving an enhancement in electron density in the high latitude ionosphere, Plasma Sci. Technol., 18, 890-896, https://doi.org/10.1088/1009-0630/18/9/03, 2016.

Wu, J., Wu, J., and Xue, Y.: The effect of the production and loss reactions on the parametric instability, International Journal of Computational Fluid Dynamics, 20, 491-496, https://doi.org/10.1080/10618560600909986, 2006.